Cold-formed Steel Sections Experimental Data Base

Dan Dubina

Mircea Georgescu

Dorina Goina

Viorel Ungureanu

Thirteenth International Specialty Conference on Cold-Formed Steel Structures
St. Louis, Missouri U.S.A., October 17-18, 1996

COLD-FORMED STEEL SECTIONS EXPERIMENTAL DATA BASE

Dan Dubina (1) Mircea Georgescu (2) Dorina Goina (3)
Viorel Ungureanu (4) Emilian Iorgovan (4)

Summary

Thin-walled cold-formed member critical load in the coupling point of overall/local buckling modes is defined, together with critical load erosion factor (ψ). A calibration method for (ψ) using an experimental database called DATACOST is presented.

1. Introduction: The ECBL Approach for Interactive Buckling of Cold-Formed Thin-walled Steel Members

Cold-formed thin-walled members are prone to local instability. Following thin walls buckling, cross-section area (A) is reduced to (A_{eff}). The reducing factor of area (Q) may be defined as: $Q = A_{eff} / A$ .On the basis of Erosion of Critical Bifurcation Load (ECBL) theory, for coupled instability modes [Gioncu, 1992], in [Dubina et al, 1995] a new approach was proposed of overall-local interactive buckling assuming the two theoretical simple instability modes that couple, in thin-walled compression members, are the Euler bar instability mode, $\overline{N}_E = 1/\sqrt{\overline{\lambda}}$ ($\overline{\lambda}$ = relative reduced member slenderness) and the local instability mode ($\overline{N}_L$) described by means of the reducing factor of area, $\overline{N}_L = Q$. The resulting eroded curve describing coupled instability mode is $\overline{N}(\overline{\lambda}, Q, \psi)$ (see Fig. 1).

Critical load maximum erosion (due to both imperfections and coupling effect) occurs in instability modes interaction point M $(\overline{\lambda} = 1/\sqrt{Q})$ where the erosion factor (ψ) is defined as:

$$\psi = \overline{N}_M - \overline{N} = \overline{N}_L - \overline{N} = Q - \overline{N} \tag{1}$$

where $\overline{N}(\overline{\lambda} = 1/\sqrt{Q}, Q, \psi)$ is the relative interactive buckling load.

(1) Professor of Structural Mechanics, Technical University of Timisoara, CMMC Department, Str. Stadion 1, RO-1900 Timisoara, Romania
(2) Senior Lecturer of Steel Structures, Technical University of Timisoara, CMMC Department, Str. Stadion 1, RO-1900 Timisoara, Romania
(3) Research Assistant, Romanian Academy, Timisoara Division, Bd. M. Viteazul 24, RO-1900 Timisoara, Romania
(4) Assistant Professor, Technical University of Timisoara, Department of Architecture, str. Traian Lalescu 2A, RO-1900 Timisoara, Romania

It must be underlined that $\overline{N}_L = Q$ is not precisely the theoretical local buckling curve, but it can be assumed (in a simplified manner, of course) as a *level* of the cross-section local buckling mode. However, Winter formula for computing effective width and Q is not a theoretical one because it was obtained in a semi-empirical way, modifying the theoretical formula given by Von Karman on the basis of experimental tests. On the other hand it is nevertheless evident that, even using Winter formula in Q computing, the fact of not considering at all the interaction between component walls of the cross-section, causes an under evaluation of the short member strength.
The Ayrton-Perry equations used to plot European buckling curves for hot-rolled members may be quite easily adapted for thin-walled cold-formed members [Dubina et al, 1995]. Dubina has shown that the following relations exist between the solutions of adapted Ayrton-Perry equations and the values of eroded coupling load, either in compression or in bending (see also fig. 1):

Compression members

$$\overline{N} = \frac{1+\alpha(\overline{\lambda}-0.2)+Q\overline{\lambda}^2}{2\overline{\lambda}^2} - \frac{1}{2\overline{\lambda}^2}\sqrt{[1+\alpha(\overline{\lambda}-0.2)+Q\overline{\lambda}^2]^2-4Q\overline{\lambda}^2} = (1-\psi)Q \tag{2}$$

Bent Members

$$\overline{M}_{LT} = \frac{1+\alpha_{LT}(\overline{\lambda}_{LT}-0.4)+Q_{LT}\overline{\lambda}_{LT}^2}{2\overline{\lambda}_{LT}^2} - \frac{1}{2\overline{\lambda}_{LT}^2}\sqrt{[1+\alpha_{LT}(\overline{\lambda}_{LT}-0.4)+Q_{LT}\overline{\lambda}_{LT}^2]^2-4Q_{LT}\overline{\lambda}_{LT}^2} = (1-\psi_{LT})\cdot Q_{LT} \tag{3}$$

In upper formulas, the following transformations may be operated:

Compression members	**Bent Members**	
$\overline{\lambda} = 1/\sqrt{Q}$	$\overline{\lambda}_{LT} = 1/\sqrt{Q_{LT}}$	(4)

which lead to:

$$\alpha = \frac{\psi^2}{1-\psi}\cdot\frac{\sqrt{Q}}{1-0.2\sqrt{Q}} \qquad \alpha_{LT} = \frac{\psi_{LT}^2}{1-\psi_{LT}}\cdot\frac{\sqrt{Q_{LT}}}{1-0.4\sqrt{Q_{LT}}} \tag{5}$$

This represents the new formula of "α" imperfection coefficient which should be introduced in European buckling curves in order to adapt these curves to overall-local buckling.

2. Experimental Approach for the Evaluation of ψ Erosion Factor

There are three distinct approaches that can be used to evaluate ψ Erosion Factor:
1. the analytical approach, that can be developed in the frame of the general theory of elastic stability, having as main goal to compute the low of axial rigidity of the related column in the vicinity of critical bifurcation point;
2. the numerical approach based on Finite Element (FEM) or Finite Strip (FSM) non-linear analysis of the behaviour of thin-walled columns in the vicinity of critical bifurcation point;
3. the experimental approach that is involving a statistical analysis of a representative series of column test results corresponding to specified cross-section shape which are characterised by means of Q factor in a *slenderness range of interactive buckling*; i.e. the vicinity of the point

$\bar{\lambda} = 1/\sqrt{Q}$ (see Fig. 2 and 3).

Due to the complexity of the first two approaches, the experimental approach seems to be the most appropriate way to evaluate the erosion factor.

This approach is performing a statistical analysis on a representative series of column test results. Specific cross-section shapes are used (characterised by means of Q factor) included in a slenderness range close to the interactive buckling point M. This range is defined by $\bar{\lambda} = 1/\sqrt{Q} \pm \varepsilon$ (see fig. 2 and 3).

If **n** tested members are available, $N_{i,exp}$ and $M_{i,exp}$ are defined as experimentally measured **i** member strengths, while $N_{i,pl}$ and $M_{i,pl}$ plastic **i** member strengths in compression and bending respectively.

Reduced member strengths in compression and bending thus results:

Compression **Bending**

$$\overline{N}_{i,exp} = \frac{N_{i,exp}}{N_{i,pl}} \qquad \overline{M}_{i,exp} = \frac{M_{i,exp}}{M_{i,pl}} \tag{6}$$

Mean value of the reduced member strength for **n** tested specimen:

$$m_{exp} = \frac{1}{n}\sum_{i=1}^{n}\overline{N}_{i,exp} \qquad m_{exp} = \frac{1}{n}\sum_{i=1}^{n}\overline{M}_{i,exp} \tag{7}$$

In figures 2 and 3 $\mathbf{m_{exp}}$ represents the mean value of reduced member strength **n** tested specimen within the *interactive buckling slenderness range* and $\mathbf{s_{exp}}$ is the standard deviation of these experimental values.

The experimental approach for (ψ) evaluation includes the following steps:

1. Compute the *individual* erosion for the **i** column specimen:

Compression **Bending**

$$\psi_i = Q_i - \overline{N}_{i,exp} \qquad \psi_i = Q_{LT,i} - \overline{M}_{i,exp} \tag{8}$$

2. Compute the mean value of ψ erosion factor for all **n** columns with the same cross-section shape, tested in the interactive buckling slenderness range:

Compression **Bending**

$$\psi_m = \frac{1}{n}\sum_{i=1}^{n}(Q_i - \overline{N}_{i,exp}) \qquad \psi_m = \frac{1}{n}\sum_{i=1}^{n}(Q_{LT,i} - \overline{M}_{i,exp}) \tag{9}$$

3. The experimental results that lead to excessively distant results from former mean value should be eliminated.

Reduced specimen series results introducing new boundaries by means of an imposed scattering for the experimental value, Δ:

$$\%\Delta = |\psi - \psi_m| / \psi_m \cdot 100 \tag{10}$$

A 50% to 70% scattering of experimental values is quite usual in structural engineering.

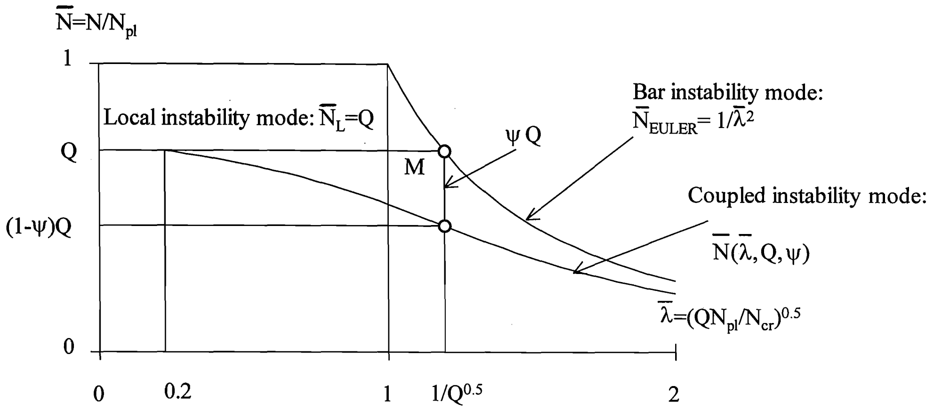

Fig 1. - The Interactive Buckling Model based on the ECBL Theory

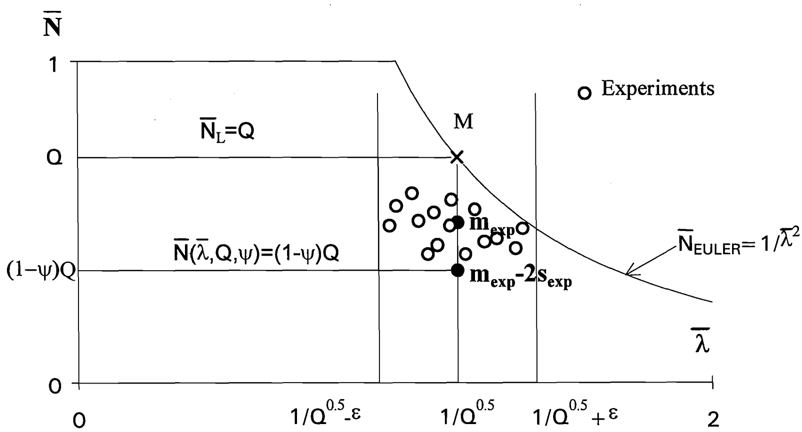

Fig. 2 - Evaluation of ψ Erosion Factor by means of experimental tests

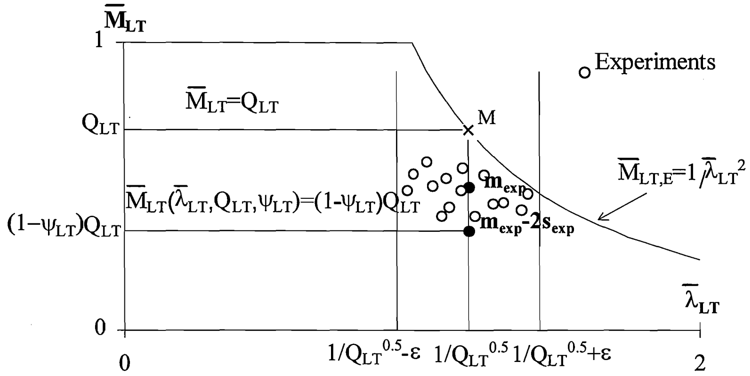

Fig. 3 - Evaluation of ψ_{LT} Erosion Factor by means of experimental tests

Only the experimental values included within this scattering limited range will be used to compute ψ_d factor.

4. A new (ψ_m) value is computed using the resulting number of $n_1 \leq n$ specimens, as well as the related standard deviation (s_ψ).

5. The design value of the erosion factor (ψ_d) results as:

$$\psi_d = \psi_m + 2s_\psi \tag{11}$$

3. Cold-formed Steel Sections Experimental Database

Current design experience has led to the observation that European buckling curves used at present for hot-rolled steel profiles are not entirely suitable for thin-walled cold-formed ones. In the same time, plotting new buckling curves by a similar experimental campaign to the one performed in Europe in the years 1970, is a difficult and expensive task. Thus, the idea has appeared of collecting all available experimental data from the field of thin-walled cold-formed (TWCF) members in the frame of a database. Using this database, together with ECBL theory and appropriate statistical processing of relevant test series, new values of the imperfection factor (α) from the European buckling curves can be obtained, adapting these curves to TWCF members.

The DATACOST package was designed within MICROSOFT ACCESS medium, taking into account the facilities offered by this software. DATACOST is including experimental data files (in the form of database tables), computation procedures for various statistical processing of stored test results, as EUROCODE 3-Part 1.3 and AISI-LRFD/1990 Design Codes. A general flow chart of DATACOST package is shown in figure 4.

At the present stage, DATACOST user should follow the next sequence:

1) Select from the Main Panel of DATACOST the problem type (Fig. 5);

2) Select the cross-section type (Fig. 6);

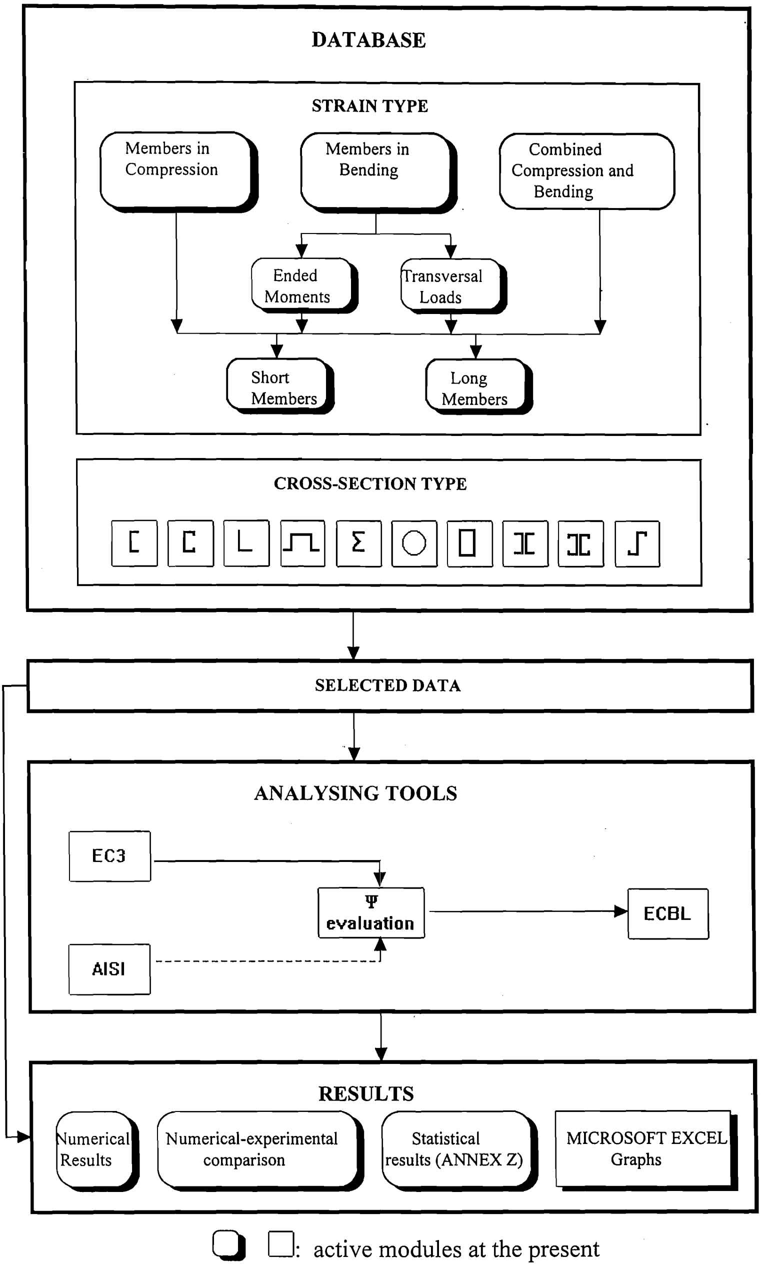

Fig. 4 - Database Flow Chart

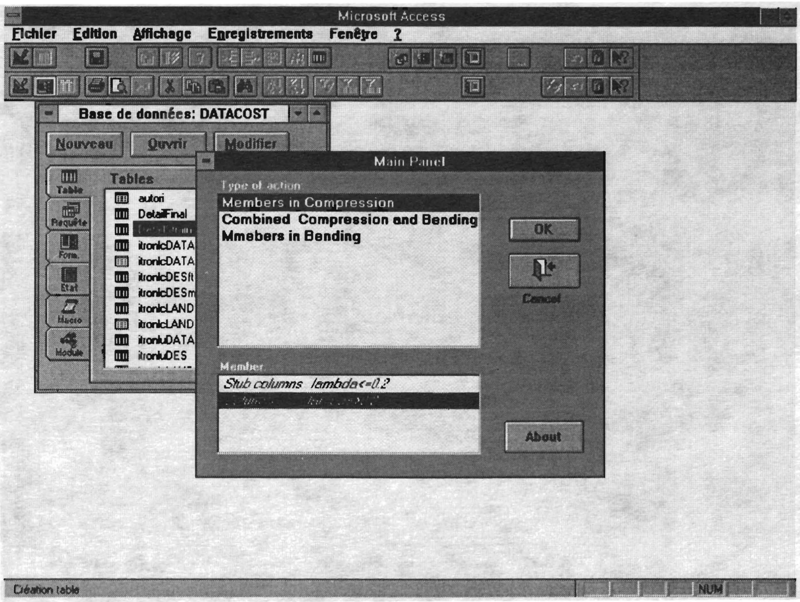
Microsoft Access
Fichier Edition Affichage Enregistrements Fenêtre ?
Base de données: DATACOST
Nouveau Ouvrir Modifier
Table Requête Form. Etat Macro Module
Tables
autori
DetailFinal
itronlcDATA
itronlcDATA
itronlcDESft
itronlcDESm
itronlcLAND
itronlcLAND
itronluDATA
itronluDES
Main Panel
Type of action
Members in Compression
Combined Compression and Bending
Mmebers in Bending
OK
Cancel
Member
Stub columns lambda<=0.2
About
Création table
NUM

Fig. 5

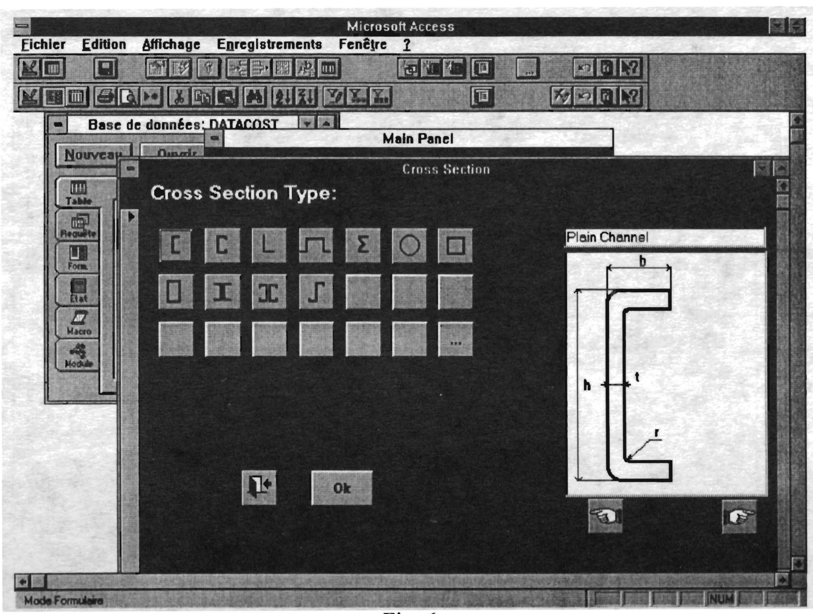
Microsoft Access
Fichier Edition Affichage Enregistrements Fenêtre ?
Base de données: DATACOST
Nouveau
Table Requête Form. Etat Macro Module
Main Panel
Cross Section
Cross Section Type:
Plain Channel
b
h
t
r
Ok
Mode Formulaire
NUM

Fig. 6

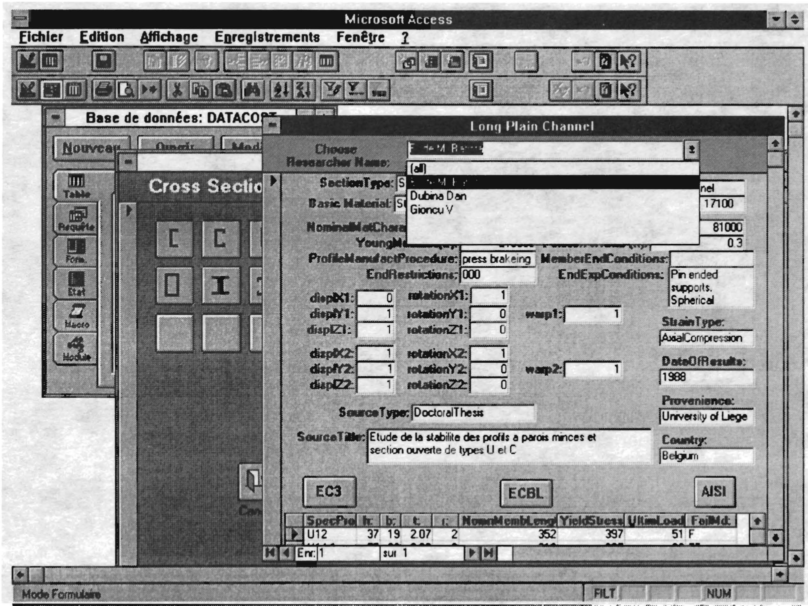
Microsoft Access
Fichier Edition Affichage Enregistrements Fenêtre ?
Base de données: DATACO
Long Plain Channel
Choose Researcher Name:
(all)
Dubina Dan
Gioncu V
Cross Sectio
SectionType:
Basic Material:
ProfileManufactProcedure: press brakeing
MemberEndConditions:
EndRestrictions: 000
EndExpConditions: Pin ended supports, Spherical
17100
81000
0.3
StrainType: AxialCompression
DateOfResults: 1988
Provenience: University of Liege
Country: Belgium
SourceType: DoctoralThesis
SourceTitle: Etude de la stabilite des profils a parois minces et section ouverte de types U et C
EC3
ECBL
AISI
SpecPro h: b: t: r: NomnMembLeng YieldStress UltimLoad FailMd:
U12 37 19 2.07 2 352 397 51 F
Enr: 1 sur 1
Mode Formulaire
FILT
NUM

Fig. 7

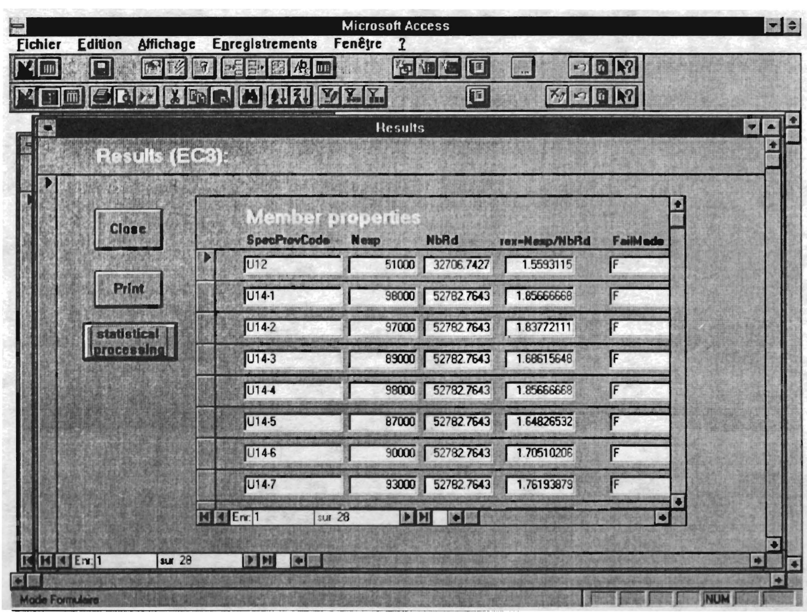
Microsoft Access
Fichier Edition Affichage Enregistrements Fenêtre ?
Results
Results (EC3):
Close
Print
statistical processing
Member properties
SpecProvCode Nexp NbRd rex=Nexp/NbRd FailMode
U12 51000 32706.7427 1.5593115 F
U14-1 98000 52782.7643 1.85666668 F
U14-2 97000 52782.7643 1.83772111 F
U14-3 89000 52782.7643 1.68615648 F
U14-4 98000 52782.7643 1.85666668 F
U14-5 87000 52782.7643 1.64826532 F
U14-6 90000 52782.7643 1.70510206 F
U14-7 93000 52782.7643 1.76193879 F
Enr: 1 sur 28
Enr: 1 sur 28
Mode Formulaire
NUM

Fig. 8

3) Experimental data file corresponding to selected specimen series is displayed. The data files may be selected following the research source or the author. The computation procedure according to ECBL, to EC3 or AISI-1990 Design Codes may be also selected (Fig. 7);
4) Gross cross-section properties obtained by processing are displayed;
5) Effective cross-section properties obtained by processing are displayed;
6) Theoretically predicted ultimate load and the ratio between theoretical and experimental ultimate load, together with the failure modes are given (Fig. 8);
7) Statistical experimental/theoretical results analysis and graphs using MICROSOFT EXCEL may be optionally requested.

4. Numerical Examples

The experimental results for columns obtained in the MSM Laboratory of the University of Liège [Batista 1987], [Rondal 1992] and at Cornell University [Weng & Pekoz, 1990] will be used in order to evidence the experimental approach for ψ factor evaluation.

In order to study erosion coefficient ψ_d change, several interaction ranges ($1/\sqrt{Q} \pm \varepsilon$), as well as scattering values were proposed. Corresponding results are presented in tables 1 to 4.

Table 1-Erosion coefficient .Specimen series: 49 channel section tested in Liege [Batista, 1987]

Scattering -Δ	30%			50%			70%		
Interaction range	ψ_m	s_ψ	ψ_d	ψ_m	s_ψ	ψ_d	ψ_m	s_ψ	ψ_d
$1/Q^{0.5} \pm 0.15$	0.249	0.043	0.335	0.261	0.080	0.421	0.247	0.089	0.425
$1/Q^{0.5} \pm 0.20$	0.193	0.038	0.269	0.208	0.068	0.344	0.208	0.068	0.344
$1/Q^{0.5} \pm 0.25$	0.193	0.038	0.269	0.185	0.062	0309	0.198	0.069	0.336

Table 2-Erosion coefficient. Specimen series: 100 lipped channel section tested in Liège [Batista, 1987]

Scattering-Δ	30%			50%			70%		
Interaction range	ψ_m	s_ψ	ψ_d	ψ_m	s_ψ	ψ_d	ψ_m	s_ψ	ψ_d
$1/Q^{0.5} \pm 0.15$	0.236	0.039	0.314	0.234	0.072	0.378	0.232	0.099	0.430
$1/Q^{0.5} \pm 0.20$	0.242	0.041	0.324	0.248	0.069	0.386	0.239	0.097	0.433
$1/Q^{0.5} \pm 0.25$	0.245	0.040	0.325	0.258	0.070	0.398	0.252	0.098	0.448

Table 3-Erosion coefficient. Specimen series: 71 lipped channel section tested at Cornell U [Weng & Pekoz, 1990]

Scattering-Δ	30%			50%			70%		
Interaction range	ψ_m	s_ψ	ψ_d	ψ_m	s_ψ	ψ_d	ψ_m	s_ψ	ψ_d
$1/Q^{0.5} \pm 0.15$	0.325	0.060	0.445	0.319	0.084	0.487	0.303	0.096	0.495
$1/Q^{0.5} \pm 0.20$	0.335	0.061	0.457	0.329	0.097	0.523	0.316	0.105	0.526
$1/Q^{0.5} \pm 0.25$	0.336	0.058	0.452	0.310	0.097	0.504	0.311	0.110	0.531

Table 4-Erosion coefficient. Specimen series: 216 hollow section tested in Liège [Rondal, 1992].

Scattering	30%			50%			70%		
Interaction range	ψ_m	s_ψ	ψ_d	ψ_m	s_ψ	ψ_d	ψ_m	s_ψ	ψ_d
$1/Q^{0.5} \pm 0.15$	0.288	0.033	0.354	0.286	0.072	0.430	0.296	0.091	0.478
$1/Q^{0.5} \pm 0.20$	0.281	0.035	0.351	0.281	0.066	0.413	0.274	0.094	0.462
$1/Q^{0.5} \pm 0.25$	0.277	0.043	0.363	0.268	0.067	0.402	0.266	0.087	0.440

It is evident from upper tables that in case of compressed members, ψ_d erosion coefficient is few sensitive in respect with interaction range $(1/\sqrt{Q} \pm \varepsilon)$ changes, but considerably influenced by scattering change (raising with scattering increase).
Studying experimental ultimate load N_{exp} relation to the theoretically predicted load N_{th} (computed by using ECBL method and ψ_d values extracted from tables 1-4) leads us to a good correlation in case of plain channel sections tested in Liege ($\rho>0.9$) respectively to a satisfactory one in case of lipped channel section tested at Cornell University and hollow section tested in Liege ($0.8< \rho <0.9$) as evident from Figures 9 to 11.
A good safety level (m-2s) results for plain channel and hollow section tested in Liege and for lipped channel section tested at the Cornell University.
In case of bent members, the experimental data carried out at the University of Salford [Lovell, 1985] and University of Strathclyde, in Glasgow [Rhodes & Harvey, 1970], [Seah, 1989], included in DATACOST, are used to evaluate ψ_{LT}.
In case of bent members the values of the erosion factor, for both lipped channel and channel section, calculated for different interaction ranges ε and scattering Δ are presented in Tables 5 and 6, respectively.

Table 5 - Values of Erosion Factor for Lipped Channel Section Beams

Rhodes Lipped Channel Section (41 Tests)									
Scattering Δ	30%			50%			70%		
Inter. range	ψ_m	s_ψ	ψ_d	ψ_m	s_ψ	ψ_d	ψ_m	s_ψ	ψ_d
$1/Q^{0.5} \pm 0.15$	0.309	0.035	0.379	0.305	0.036	0.376	0.302	0.034	0.371
$1/Q^{0.5} \pm 0.20$	0.309	0.035	0.379	0.314	0.046	0.407	0.320	0.052	0.424
$1/Q^{0.5} \pm 0.25$	0.291	0.068	0.428	0.299	0.072	0.442	0.308	0.071	0.450
Lovell's Lipped Channel Section (27 Tests)									
$1/Q^{0.5} \pm 0.15$	0.233	0.039	0.311	0.233	0.039	0.311	0.224	0.037	0.297
$1/Q^{0.5} \pm 0.20$	0.238	0.078	0.394	0.211	0.055	0.321	0.231	0.072	0.374
$1/Q^{0.5} \pm 0.25$	0.238	0.078	0.394	0.213	0.092	0.398	0.234	0.103	0.440

Table 6 - Values of Erosion Factor for Lovell's Channel Tests (20 Tests)

Scattering Δ	30%; 50%; 70%		
Interaction range	ψ_m	s_ψ	ψ_d
$1/Q^{0.5} \pm 0.20$	0.226	0.015	0.256
$1/Q^{0.5} \pm 0.25$	0.199	0.048	0.294

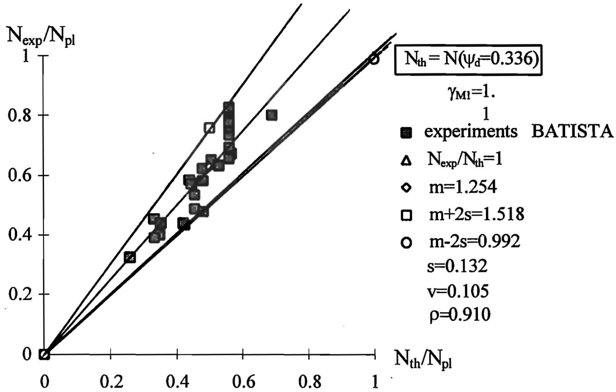

Figure 9 - Relation between N_{exp} and N_{th} - Channel Section - Liège/Belgium

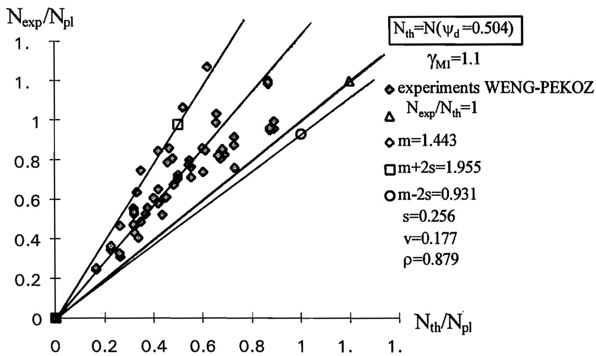

Figure 10 - Relation between N_{exp} and N_{th} - Lipped Channel Section - Cornell University/

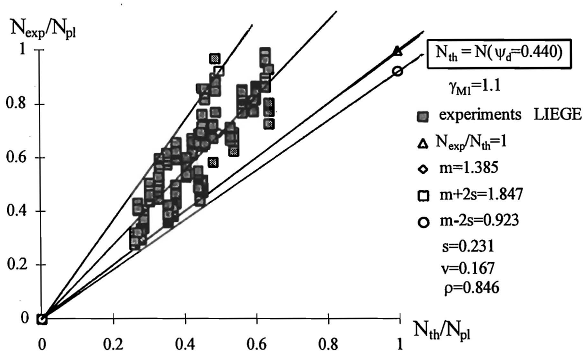

Figure 11 - Relation between N_{exp} and N_{th} - Hollow Section - Liège/Belgium

Studying experimental ultimate bending moment M_{exp} relation to the theoretically predicted ultimate bending moment M_{th} (computed by using ECBL method and ψ_d values extracted from table 5), leads us to good correlation, respectively to good security levels in case of lipped channel sections tested at Salford University, as evident from figures 12 and 13.
Tables 6 and 7 give comparatively the two series of α values to be used for cold-formed lipped channel section columns corresponding to EC3 and ECBL approach.

TABLE 6 - Values of α imperfection factor to be used in interactive buckling of Cold-formed Lipped Channel Section Columns

Method	Compression Lipped Channel Sect.(Batista) $\psi_d = 0.448$	Compression Lipped Channel Sect. (Weng-Pekoz) $\psi_d = 0.504$	Compression Channel (Batista) $\psi_d = 0.336$	Compression Hollow Sect. (Rondal) $\psi_d = 0.440$
	Q=0.686	Q=0.820	Q=0.618	Q=0.638
α - EC3	0.34	0.34	0.49	0.49
α - ECBL	0.361	0.566	0.159	0.329

TABLE 7 - Values of α_{LT} imperfection factor to be used in interactive buckling of Cold-formed Lipped Channel Section Beams

Method	Compression Lipped Channel Sect. (Rhodes) $\psi_d = 0.376$	Compression Lipped Channel Sect. (Lovell) $\psi_d = 0.321$	Compression Channel (Lovell) $\psi_d = 0.256$
	Q_{LT}=0.524	Q_{LT}=0.761	Q_{LT}=0.531
α_{LT} - EC3	0.21	0.21	0.21
α_{LT} - ECBL	0.231	0.203	0.092

Typical buckling curves plotted using ECBL method, for compression channel and hollow sections and for bent channel and lipped channel sections are presented in figures 14 to 17. A comparison is made with the corresponding buckling curves plotted using European code EUROCODE 3-Part 1.3 and also with experimental values.

5. Concluding Remarks

1. Only database fundamental principles and some illustrating examples have been given in the present paper, since its building is still an ongoing process.
2. On authors' opinion, such a database (in connection with ECBL method) could solve in a very economic way the buckling curves problem for thin-walled cold-formed profiles.
3. Concerning ECBL method generality, as distorsional buckling mode is modelled at the present time by a conventional equivalent width, the method seems to apply on the coupling between overall (member) buckling and distorsional buckling also.
4. From the very beginning, DATACOST was intended to be an open expert system and a continuously developing one, especially concerning the following topics: data acquisition; computation modules; statistical processing; interface with a FEM or FSM numerical simulation computer code.

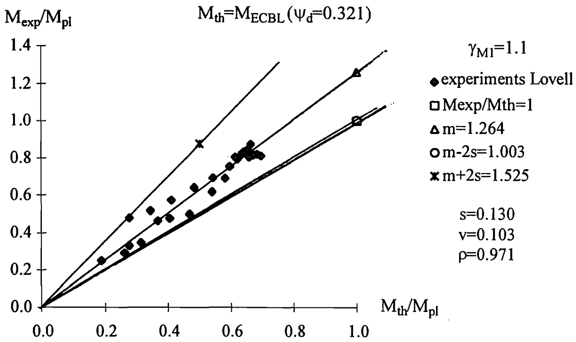

Figure 12 - Relation between M_{exp} and M_{th}- Channel Section - Salford University

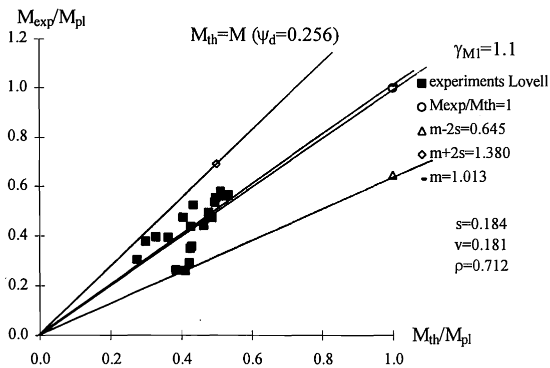

Figure 13 Relation between M_{exp} and M_{th} - Lipped Channel Section - Salford University

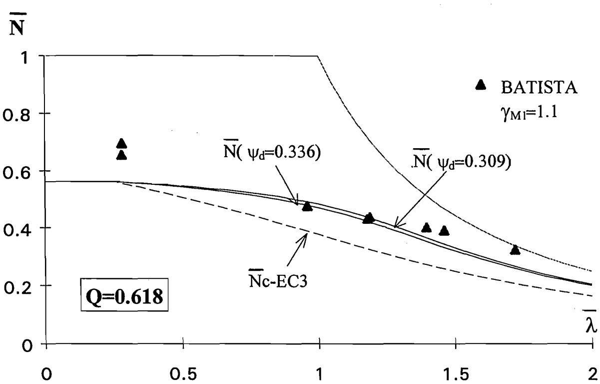

Fig. 14 - EC3 and ECBL Buckling Curves: Channel Section Columns

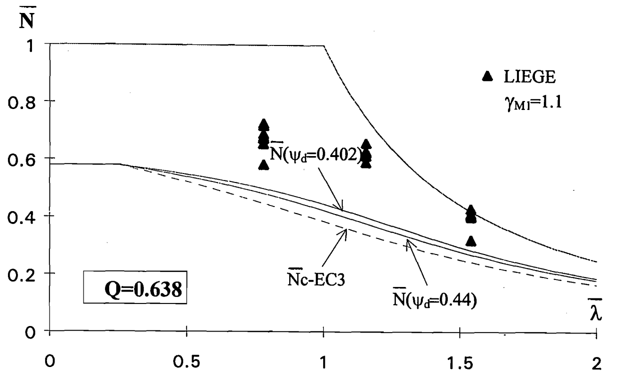

Fig. 15 - EC3 and ECBL Buckling Curves: Hollow Section Columns

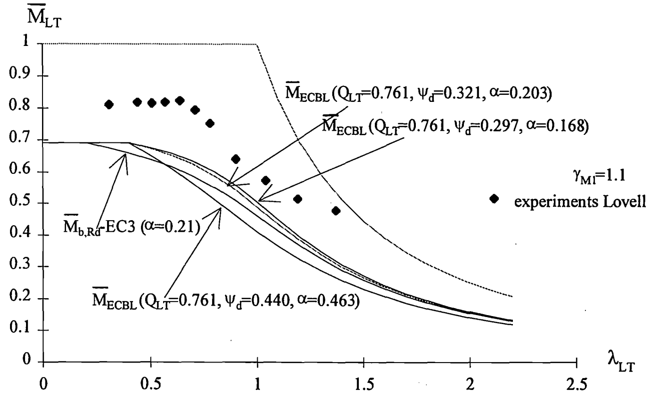

Fig. 16 - EC3 and ECBL Buckling Curves: Lipped Channel Section Beams

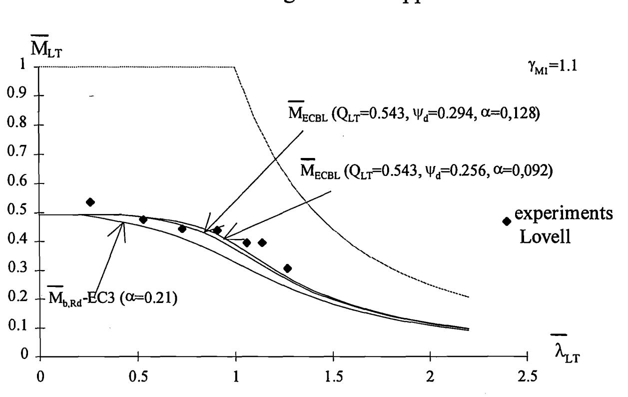

Fig. 17 - EC3 and ECBL Buckling Curves: Channel Section Beams

However, the purpose of building such a complex expert system cannot be reached by a single research team only, mainly concerning the acquisition of experimental data. *We are thus inviting all interested research teams to join us in the frame of an international co-operation by providing us their experimental results in the field of TWCF steel members. All participating teams in this international co-operation will freely benefit of the product use.*

Though initially built as a logistic support in plotting specific buckling curves for TWCF steel members based on ECBL theory, DATACOST has much larger possibilities as:

-the benefit of a large accumulated volume of experimental data;

-theoretical prediction of compression/bent member strength according either to EUROCODE 3-Part 1.3 or to AISI LFRD Design Codes;

-various numerical comparisons and statistical processing of included data.

7. ACKNOWLEDGEMENTS

The authors gratefully acknowledge the contribution with experimental data in DATACOST of Prof. Jacques Rondal from the University of Liège, Dr. Eduardo de Miranda Batista from Federal University of Rio de Janeiro, Prof. Jim Rhodes from Strathclyde University of Glasgow, Prof. Gregory Hancock from University of Sydney and Prof. Joachim Lindner from Technical University of Berlin.

Appendix.--Notation

A	gross cross-section area
A_{eff}	effective cross-section area
$\overline{N} = N / N_{pl}$	relative axial load
N	axial load
N_E	Euler critical buckling load
$\overline{N}_E = N_E / N_{pl}$	relative Euler critical buckling load
N_{exp}	experimental member strength in compression
N_{pl}	full plastic resistance of the column
$\overline{N}_{exp} = N_{exp} / N_{pl}$	relative experimental member strength in compression
N_L	local buckling load
$\overline{N}_L = N_L / N_{pl}$	relative local buckling load
N_{th}	theoretically predicted value of ultimate load
M_{cr}	the elastic critical moment for lateral torsional buckling for the gross cross-section
M_{exp}	experimental member strength in bending
Mpl	full plastic moment
$\overline{M}_{exp}$	relative experimental member strength in bending
$\overline{M}_{LT} = M / M_{pl}$	relative bending moment

M_{th}	theoretically predicted value of ultimate moment
m	the mean value of N_{exp}/N_{th} ratios or M_{exp}/M_{th} ratios
$Q = A_{eff} / A$	reducing factor of area in interactive local-overall buckling
$Q_{LT} = W_{eff} / W_{pl}$	reducing factor of section modulus in interactive local-lateral torsional buckling
s	the standard deviation related to N_{exp}/N_{th} ratios or M_{exp}/M_{th} ratios, respectively
s_{ψ}	the standard deviation related to ψ_i and ψ_m values
v	coefficient of variation related to N_{exp}/N_{th} and M_{exp}/M_{th} ratios respectively
W_{eff}	section modulus of the effective cross-section when subject only to moment about relevant axis
W_{pl}	the full plastic section modulus of the cross-section
α	imperfection coefficient for compression members
α_{LT}	imperfection coefficient for bent members
Δ	scattering of experimental results
ε	interaction range
γ_{M1}	partial safety factor
$\bar{\lambda} = \sqrt{Q \cdot N_{pl} / N_{cr}}$	reduced relative member slenderness for compression members
$\bar{\lambda}_{LT} = \sqrt{Q_{LT} \cdot M_{pl} / M_{cr}}$	reduced relative member slenderness for bent members
ρ	correlation factor between experimental and theoretical results
ψ	erosion factor for compression members
ψ_{LT}	erosion factor for bent members
ψ_m	the mean value of ψ erosion factor for a given series of experimental data
ψ_d	design value of erosion factor

Appendix.--References

Batista, E.M., 1987, “Essais de profils C et U en acier plies à froid”, Laboratoire MSM, Université de Liège, Rapport No. 157.

Dubina D. et al, 1995, "Interactive buckling of cold-formed thin-walled members", Structural Stability and Design, ed. Kitipornchai S., Hancock G.J. & Bradford M.A. (Balkema, Rotterdam), 49-54.

Gioncu, V., 1992, “General Theory of Coupled Instabilities”, General Report, Proceedings of “Coupled Instabilities in Metal Structures” Conference, Timisoara, Romania, Elsevier Applied Science, Thin-Walled Structures, Volume 19, Nos 2-4 1994, pp.81.

Lovell M.H., 1985, “Lateral buckling of light gauge steel beams”, Research Report, Department of Civil Engineering, University of Salford.

Rhodes, J.; Harvey, J.M., 1970, Scientific Paper, Proc. of The Fourth Conference on Experimental Stress Analysis, pp. 15.

Seah L.K., 1989, “Buckling Behaviour of Edge Stiffeners in Thin-Walled Sections”, Doctoral Thesis.

Weng, C.C.; Pekoz, T., 1990, “Compression Tests of Cold-Formed Steel Columns”, ASCE, Journal of Structural Engineering, Vol. 116, Nr. 5.